Resonating Electrostatically Guided Electrons

M. Seidling,[1,*] F. D. F. Schmidt-Kaler,[1,*,†] R. Zimmermann,[1] J. W. Simonaitis,[2]
P. D. Keathley,[2] K. K. Berggren,[2] and P. Hommelhoff[1]
[1]Department of Physics, Friedrich-Alexander-Universität Erlangen-Nürnberg (FAU),
Staudtstrasse 1, D-91058 Erlangen, Germany
[2]Research Laboratory of Electronics, Massachusetts Institute of Technology,
Cambridge, Massachusetts 02139, USA

(Received 28 August 2023; revised 20 December 2023; accepted 2 May 2024; published 17 June 2024)

An essential component for quantum-enhanced measurements with free electrons is an electron resonator. We report stable guiding of free electrons at 50 eV energy for up to seven round trips in a linear autoponderomotive guiding structure, which is realized with two microstructured printed circuit boards that generate the required electromagnetic fields. Free electrons are laser triggered from a sharp tungsten needle tip and coupled in at the front of the electron resonator with the help of sub-nanosecond-fast switchable electron mirrors. After a variable time delay, we open the rear electron mirror and measure the number of trapped electrons with a delay-line detector. We demonstrate, simulate, and show ways of optimizing an electron resonator in simulations, which will help enable "interaction-free" measurement setups, including multipass and quantum-Zeno effect based schemes, helping to realize the quantum electron microscope.

DOI: 10.1103/PhysRevLett.132.255001

Electron microscopy relies on one-time electron-sample interaction. The success of this imaging modality has been tremendous, a recent example being the spectacular surge of cryoelectron microscopy, which has enabled atomic resolution of biologically relevant molecules [1,2]. However, even this imaging technique cannot record an image of one individual molecule with atomic resolution as the electron beam destroys the sample before sufficient information can be gained [3]. Hence, many molecules of the same type are partially imaged, the results of which are processed with computational algorithms.

To enable the imaging of damage-sensitive specimens and to facilitate true single-particle imaging, new imaging methods must be developed. One of them is multipass imaging, which relies on a single electron interacting with the sample multiple times and thereby accumulating a larger phase shift than just with a single passage [4]. Another proposed scheme is the interaction-free measurement, which is based on the quantum Zeno effect, where the electron interrogates the sample multiple times [5–8]. An interaction-free measurement has been realized with photons [9] and a first step has been taken with a single pass "interaction-free" measurement with electrons [10]. An enhancement resonator for multiple reflections is key in achieving sufficiently high efficiency. Here, we demonstrate a first electron resonator for electrons having a central energy of 50 eV: we show controlled and repeated reflection of electrons and measure the coupling efficiency to the mode, which is an important step toward coherent electron beam manipulation. Our approach can be directly scaled up to 5 keV [11,12] and is directly applicable with minor changes.

Our resonator relies on the principle of the electrodynamic Paul trap, that features a stable ion confinement in three dimensions, see Fig. 1(a) and [13,14] and has been shown to work for electrons likewise [15–17]. Technical limitations in driving frequencies of Paul traps, in turn, limiting the maximally guidable electron energy led us to pioneer the use of a static electric potential from micro-segmented electrodes. Here, the moving electron with velocity v_z samples a polarity, altering at a period length L_P that generates an autoponderomotive radially confining Paul-trap-like pseudo-potential, see Figs. 1(c) and 1(d). The electron motion-induced autoponderomotive angular driving frequency ω then results as

$$\omega = \frac{2\pi v_z}{L_\mathrm{P}}. \tag{1}$$

We optimize the autoponderomotive geometry and voltage for guiding of up to 5 keV electron energies, see Refs. [11,12].

To form a resonator for electron bunches, a linear autoponderomotive guiding structure is complemented with switchable mirrors at both ends. The experimental setup is comprised of (i) a laser-triggered source for electron bunches, which are injected into the resonator formed by (ii) a switchable input mirror, (iii) an electrostatic autoponderomotive electron guide, and (iv) a switchable output mirror. The transmitted electron bunches are recorded on a (v) delay line detector (DLD).

As an electron source (i), we employ a tungsten needle emitter biased with the acceleration voltage U_A, and an

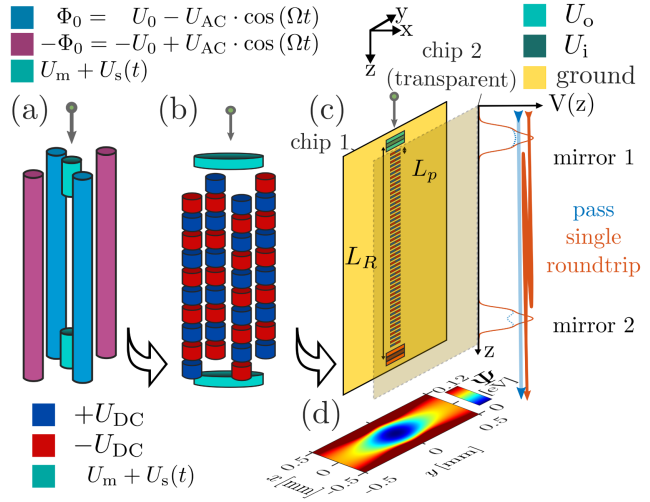

FIG. 1. (a) Sketch of a conventional, fully three-dimensional linear Paul trap with switchable end-cap mirrors on either side. (b) The electrostatic counterpart of the conventional radio-frequency-driven or microwave-driven system makes use of segmented electrodes at *static* potentials. This concept works for electrons moving up and down between the end caps: in the frame of the moving electron, these static fields transform into an alternating potential, forming the transverse autoponderomotive electron trapping potential. (c) Chip-based, planar realization of the structure shown in (b) based on two opposing substrates with the electrodes projected onto them. The second chip (chip 2) is indicated transparently to provide a clearer view of the electrode layout. (d) Autoponderomotive potential in the linear guiding part of the resonator, not to scale [the yellow substrate in (c) is ~6 cm wide, for reference]. Guiding of electrons with an energy of up to 5 keV has been demonstrated in a comparable autoponderomotive structure [11,12]. In this Letter, we demonstrate that such a guide can be transformed to work as a resonator by adding switchable end-cap electron mirrors, the electrodes for which are shown in green (top) and red (bottom). The electron mirrors each consist of three electrodes at static potentials with the central one fed with a fast switching signal of a homebuilt GaN FET pulser situated next to each mirror (see Supplemental Material [18]). This central potential provides the mirror potential, which can be quickly switched on and off. Right next to the planar chips, we show the simulated mirror potentials $V(z)$ in the open state (blue) and closed state (orange). The blue arrow indicates straight electron transmission with both mirrors open, whereas the orange path depicts one round trip, for which both mirrors have to be switched in a sequence as discussed in the main text and outlined in Fig. 2(b). More details including pictures of the resonator can be found in Supplemental Material [18].

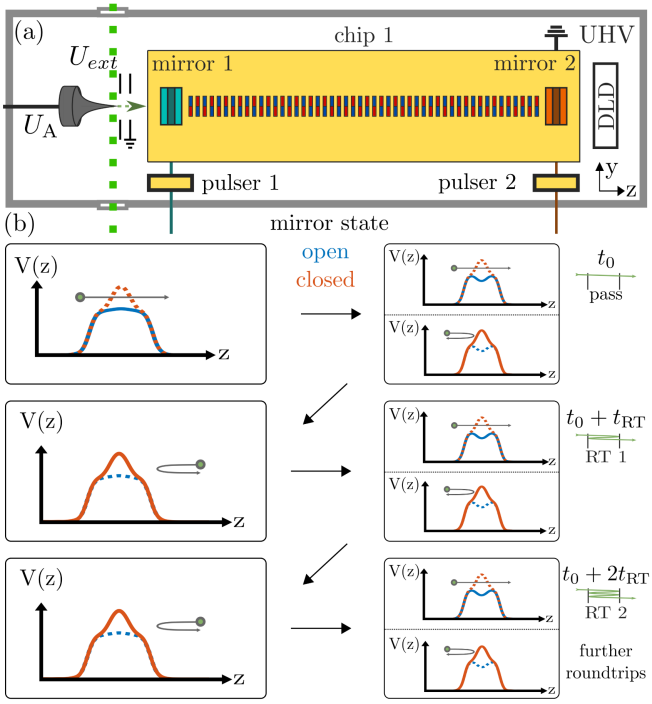

FIG. 2. (a) Sketch of the experimental setup consisting of, from left to right, a femtosecond laser-triggered electron source, extractor, and ground aperture, the on-chip resonator, and the delay-line detector (DLD) inside of an ultrahigh vacuum chamber. A pulsed laser beam illuminates a tungsten tip biased at $U_A = -50$ V to generate electrons with 50 eV kinetic energy. (b) Mode of operation: electrons enter the resonator via mirror 1 (open) and can either pass mirror 2 at t_0 (upper case in the right box). A straight pass is performed. Alternatively, the electrons reflect from mirror 2 when it is closed at $t = t_0$ (lower case). If the electrons return to mirror 1, they reach it at $t_0 + \frac{1}{2}t_{RT}$. Mirror 1 is already closed and the incoming electrons are reflected. When the electrons reach the second mirror again, they can be coupled out of the resonator, by opening mirror 2 at $t_0 + t_{RT}$. We refer to this as 1 round trip, even though the electrons have passed the resonator 3 times. Alternatively, if no voltage pulse is applied to mirror 2, the electrons are reflected back to the still-closed mirror 1 to perform an arbitrary amount of further round trips.

extractor voltage U_{ext} set to suppress field emission, see Fig. 2. A pulsed laser beam triggers electrons from the tungsten needle tip and generates electron pulses [19–21]. The high voltage pulses for the electron mirrors are generated in a pulse generator with a minimal switching time of 10 ns, see Supplemental Material [18]. The laser pulses at a central wavelength of 515 nm and an energy of ~5.2 nJ are derived from a frequency-doubled ytterbium femtosecond fiber laser running at 1 MHz pulse repetition frequency with a pulse duration of < 400 fs. This generates a pulsed electron beam with an energy of $eU_A = 50$ eV and an energy spread of 0.7 eV, leading to an electron pulse length of about 1 ns measured by time-of-flight evaluation at the DLD.

The switchable electrostatic mirrors [(ii) and (iv)] on each end of the autoponderomotive guide consist of three electrodes with a width of 8 mm (y direction) and a length of 1.3 mm (z direction), see Fig. 1(c). These three mirror electrodes are separated from each other by 0.25 mm, creating a charged particle mirror of 4.9 mm depth in the z direction. The outer electrodes U_i and U_o are on a constant potential. Each central mirror electrode is supplied with a combination of a constant voltage U_m and a time-dependent switching

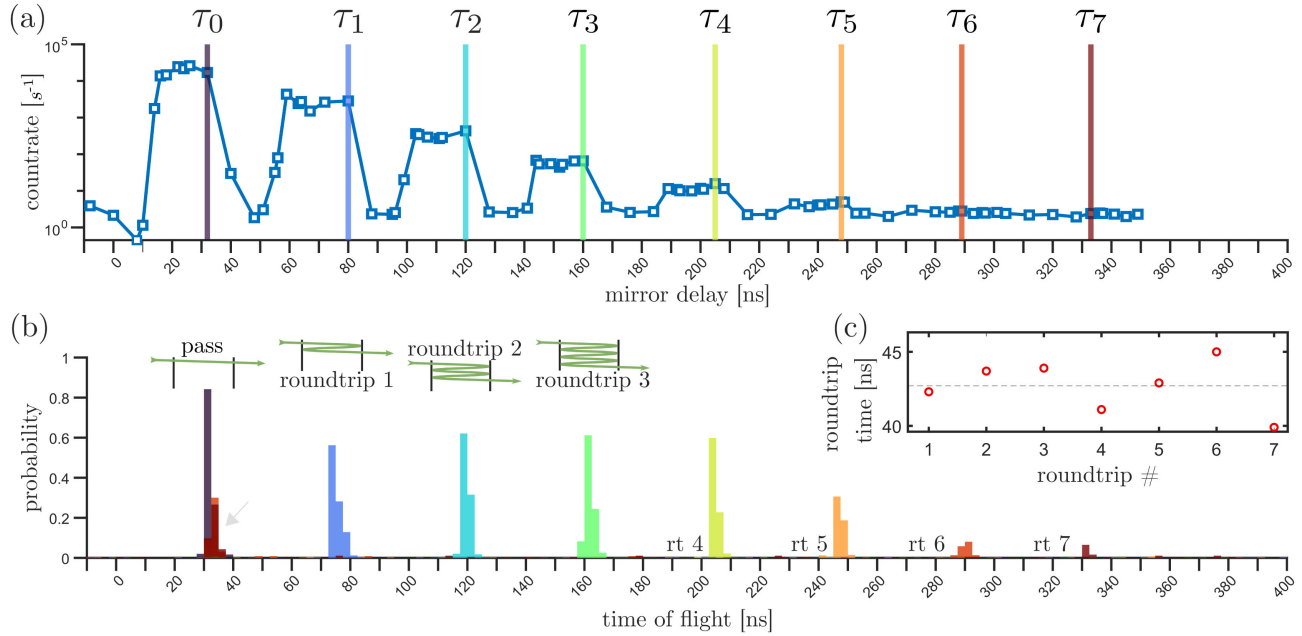

FIG. 3. Electron resonator results. (a) Electron count rate depicted as a function of the opening time of mirror 2, i.e., of the mirror delay time τ. It takes the electrons about 10 ns to arrive from the tip at the resonator entrance (first mirror) and about 20 ns to cross the resonator. The mirror operation takes about 10 ns, see Supplemental Material [18]. The first electron peak results from the electrons passing the resonator in transmission mode at $\tau = (32.5 \pm 0.2)$ ns, i.e., mirror 2 just acts as a temporal filter for the incoming electrons. The electron count rate is high, as a lot of electrons do not get coupled into the resonator and create a high secondary electron background. It is lowered at 10 ns due to mirror jitter hindering electrons from coupling into the resonator and crosstalk to the DLD shortly reducing its sensitivity (dip at 10 ns). The detector's background count rate without mirror operation is $>$ 2–4 counts/s. After that, the electrons have to perform a single round trip, which is reflected by the peak at (74.8 ± 0.2) ns. The blue line labeled τ_1 displays the first round trip [it is obtained from panel (b) right below]. The subsequent peaks correspond to more round trips, with matching colors for mirror delay (a) and the respectively recorded time-of-flight spectrum (b). We note that the equidistant peak heights shrink less than exponential with each round trip, which is mainly due to loss at the mirrors (see text and Supplemental Material [18] for details). (b) Time-of-flight spectra recorded at each respective mirror delay τ_i with $i \in [0 \ldots 7]$ with a value in bin standardized with the sum of all bins as probability. The colors correspond to the colors in panel (a): for instance, the first peak results from a time of flight measurement with $\tau = (32.5 \pm 0.2)$ ns, the second peak from $\tau = (74.8 \pm 0.2)$ ns, and so on. The insets show electron trajectories for up to three round trips. Unwanted mirror 2 leaks are marked by the faint gray arrow. (c) Fitted maxima position from panel (b). We clearly see an equidistant peak distribution with increasing mirror delay τ, evidencing a nearly constant round-trip time of $\bar{T}_{\mathrm{RT}} = (42.7 \pm 1.7)$ ns.

voltage U_{s}. The resulting mirror potentials in on and off state are indicated in both Figs. 1(c) and 2(b). We employ homebuilt high voltage GaN FET pulsers [22] supplying the central electrode of the electron mirrors with static voltages U_{m} of up to -1000 V bias and a time-dependent pulse with an amplitude U_{s} of up to $+80$ V.

For the autoponderomotive Paul-trap-like guide (iii) in between the electron mirrors confining the electrons transversely, two rows of 80 rectangular electrodes are placed in the center of both chips. Each electrode has a width (y direction) of 1.3 mm and a length (z direction along which the electrons propagate) of 0.4 mm. They are separated by 0.6 mm (z direction), which leads to a period length of $L_{\mathrm{p}} = 2$ mm. A grounded metal coating surrounds them at a distance of 100 μm to prevent charging of the nonconductive FR4 carrier substrate. Neighboring electrodes are supplied with the two constant guiding voltages $\pm U_{\mathrm{dc}}$ along the z direction typically in the range of several 10 V up to several hundred volts.

After the output mirror is opened, the electron bunches are recorded at a RoentDek delay-line detector (v) with a time resolution of < 1 ns and spatial resolution <0.1 mm [23]. All this results in a $L_{\mathrm{R}} = 87.95$ mm long electron resonator.

In the experiment, the 50 eV electron pulses are fed into the resonator potential with electrostatic double deflectors. Initially, the relative timing of the voltage dip opening the input mirror is optimized toward the laser pulse for optimal electron transmission. This input mirror delay is kept constant throughout the measurement and needs adjustment only when we vary the electron energy eU_{A}. With the output mirror closed, the electrons are reflected back to the input mirror, which by the return of the electrons at its position has been switched to a closed state as well, see Fig. 2(b). Hence, the electrons also turn around at the input mirror to again travel in positive z direction toward the detector.

By varying the opening and closing times of output mirror with respect to the laser pulse and the fixed time

delay of the input mirror, we can store the electrons for an arbitrary amount of time τ and thus round trips in the resonator. We can now vary when we open the outcoupling mirror (mirror 2), which we do after an arbitrary time delay τ with respect to the opening time of the in-coupling mirror (mirror 1). The electrons are coupled out of the resonator when the output mirror's potential is lowered. Their transverse position and arrival time are recorded at the DLD.

In the measurement, we vary the electron mirror 2 delay τ and thus storage time from -10 ns to 349 ns, see Fig. 3. We observe clear equidistantly spaced maxima of electrons on the DLD, corresponding to the increasing number of round trips of the electrons.

To gain more insights, we can record a time-of-flight measurement for each specific τ, i.e., the time between opening mirror potentials 1 and 2. We start the time-of-flight counter with the laser pulse triggering the electron emission and stop it when an electron hits the detector.

The time-of-flight results are shown in Fig. 3(b). We observe eight distinct maxima, again corresponding to the increasing number of round trips of the electrons in the resonator, starting with direct transmission of the electrons through the resonator appearing fully open after 32.5 ns. The peak at 74.8 ns time-of-flight corresponds to the first round trip inside of the resonator, 118.6 ns to two round trips, 162.4 ns to three, and so on. Up to seven electron round trips have been detected. The count rate decays in a less-than-exponential fashion, and we measure an average in- and outcoupling loss of 75% per round trip from the data shown in Fig. 3(a) and in Supplemental Material, Fig. 1.

We obtain the resonator round-trip time by evaluating the differences of the optimum mirror delays τ of the voltage pulses opening the mirror. In this way, we measure a mean round-trip time of $\bar{T}^{*}_{\mathrm{RT}} = (43.8 \pm 4.8)$ ns. Using the center of the peaks in the time-of-flight measurements using a Gaussian fit leads to an even more precise result: $\bar{T}_{\mathrm{RT}} = (42.7 \pm 1.7)$ ns. Slight variations might be induced by unwanted acceleration due to not fully decayed electric field transients from fast GaN FET pulser's switching. Both results are in excellent agreement with the expected result of $T_{\mathrm{RT}} = L_{\mathrm{R}}/v_z = (41.9 \pm 0.4)$ ns for 50 eV electrons and a resonator length of $L_{\mathrm{R}} = 87.95$ mm.

We model the details of the electron trajectories at the coupling into the guide, the mirror reflection, and inside the guide with the commercial software COMSOL and CPO [24]. From these particle tracking simulations, we infer that the highest number of round trips requires an electron beam alignment better than 20 μm with respect to the resonator axis. In addition, if the electron trajectory enters the resonator under an angle of $\leq 1°$, the maximum number of round trips is three. With a simulated collimated 2-μm beam, we find a significantly reduced loss of around 8% per round trip; see Supplemental Material [18], Fig. 1. This indicates that the resonator incoupling puts stringent requirements on the electron beam. However, most of the electron losses are due to imperfect electron trajectories in y direction after reflection from the mirrors, such that most electrons are lost in the $\pm y$ direction and almost none inside the guide or in x direction, see Supplemental Material [18], Fig. 6. The simulation and its results are discussed in more detail in Supplemental Material [18].

To summarize, we demonstrate the first linear autoponderomotive resonator for 50 eV electrons, trapping them for up to 7 round trips, which amounts to a trapping length of about 1.4 m. As the preferred direction in our autoponderomotive guiding structure renders this task nontrivial, our results represent a substantial step toward a guided electron resonator with long electron storage finesse (many round trips). For the first time, the in- and outcoupling loss into the mode could be measured to be 75% in qualitative agreement with detailed charged particle simulations. In comparison, the first multireflection time-of-flight ion mass spectrometer achieved three round trips with an average loss of 57% [25]. Today's multireflection time-of-flight ion mass spectrometers are capable of measuring a mass spectrogram after 600 round trips [26,27]. Based on this Letter, we aim to improve the mirror geometry using on-chip lenses to reduce round-trip losses. Additional simulations showed improvement for a smaller electron input beam of 2 μm opening another potential vector of approach toward a better resonator. With an increased resonator length, it could be operated up to electron energies of 1 keV using even the same GaN FET pulsers. With other geometries, we expect much higher high voltage breakdown limits, rendering this scheme scalable to higher electron energies well suited for imaging applications. Last, with an elevated mirror electrode, we expect further improved resonator behavior. These improved resonators are key for quantum-enhanced measurement protocols for electrons, like interaction-free measurement in the quantum electron microscope or multipass transmission electron microscopy. The grounded spaces between the guiding structure, which reduce the height and apparent driving frequency, are placeholders for possible insertion positions of samples. The technical realization is subject to future experiments. We also foresee these resonators to enable complex electron wave function shaping due to repeated laser interaction and quantum interference [28,29].

The authors acknowledge funding from the Gordon and Betty Moore Foundation via Grant No. 5723 (Quantum Electron Microscope Project) and No. 11473 (Imaging quantum coherence with shaped electrons), and ERC Grants No. 616823 (NearFieldAtto) and No. 884217 (AccelOnChip).

*These authors contributed equally to this work.
†Corresponding author: franz.schmidt-kaler@fau.de

[1] J. Dubochet, On the development of electron cryo-microscopy (Nobel lecture), Angew. Chem., Int. Ed. **57**, 10842 (2018).
[2] R. Henderson, From electron crystallography to single particle CryoEM (Nobel lecture), Angew. Chem., Int. Ed. **57**, 10804 (2018).
[3] R. M. Glaeser, How good can cryo-electron microscopy become?, Nat. Methods **13**, 28 (2016).
[4] T. Juffmann, S. A. Koppell, B. B. Klopfer, C. Ophus, R. M. Glaeser, and M. A. Kasevich, Multi-pass transmission electron microscopy, Sci. Rep. **7**, 1699 (2017).
[5] A. C. Elitzur and L. Vaidman, Quantum mechanical interaction-free measurements, Found. Phys. **23**, 987 (1993).
[6] P. G. Kwiat, A. G. White, J. R. Mitchell, O. Nairz, G. Weihs, H. Weinfurter, and A. Zeilinger, High-efficiency quantum interrogation measurements via the quantum Zeno effect, Phys. Rev. Lett. **83**, 4725 (1999).
[7] W. P. Putnam and M. F. Yanik, Noninvasive electron microscopy with interaction-free quantum measurements, Phys. Rev. A **80**, 040902(R) (2009).
[8] P. Kruit, R. Hobbs, C.-S. Kim, Y. Yang, V. Manfrinato, J. Hammer, S. Thomas, P. Weber, B. Klopfer, C. Kohstall, T. Juffmann, M. Kasevich, P. Hommelhoff, and K. Berggren, Designs for a quantum electron microscope, Ultramicroscopy **164**, 31 (2016).
[9] P. Kwiat, H. Weinfurter, T. Herzog, A. Zeilinger, and M. A. Kasevich, Interaction-free measurement, Phys. Rev. Lett. **74**, 4763 (1995).
[10] A. E. Turner, C. W. Johnson, P. Kruit, and B. J. McMorran, Interaction-free measurement with electrons, Phys. Rev. Lett. **127**, 110401 (2021).
[11] R. Zimmermann, M. Seidling, and P. Hommelhoff, Charged particle guiding and beam splitting with autoponderomotive potentials on a chip, Nat. Commun. **12**, 390 (2021).
[12] M. Seidling, R. Zimmermann, and P. Hommelhoff, Chip-based electrostatic beam splitting of guided kiloelectron volt electrons, Appl. Phys. Lett. **118**, 034101 (2021).
[13] W. Paul, Electromagnetic traps for charged and neutral particles, Rev. Mod. Phys. **62**, 531 (1990).
[14] J. D. Prestage, G. J. Dick, and L. Maleki, New ion trap for frequency standard applications, J. Appl. Phys. **66**, 1013 (1989).
[15] J. Hoffrogge, R. Fröhlich, M. A. Kasevich, and P. Hommelhoff, Microwave guiding of electrons on a chip, Phys. Rev. Lett. **106**, 193001 (2011).
[16] J. Hoffrogge and P. Hommelhoff, Planar microwave structures for electron guiding, New J. Phys. **13**, 095012 (2011).
[17] C. Matthiesen, Q. Yu, J. Guo, A. M. Alonso, and H. Häffner, Trapping electrons in a room-temperature microwave paul trap, Phys. Rev. X **11**, 011019 (2021).
[18] See Supplemental Material at http://link.aps.org/supplemental/10.1103/PhysRevLett.132.255001for simulated resonator trajectories and detailed comparison between measurement and simulation.
[19] P. Hommelhoff, Y. Sortais, A. Aghajani-Talesh, and M. A. Kasevich, Field emission tip as a nanometer source of free electron femtosecond pulses, Phys. Rev. Lett. **96**, 077401 (2006).
[20] P. Hommelhoff, C. Kealhofer, and M. A. Kasevich, Ultrafast electron pulses from a tungsten tip triggered by low-power femtosecond laser pulses, Phys. Rev. Lett. **97**, 247402 (2006).
[21] C. Ropers, D. R. Solli, C. P. Schulz, C. Lienau, and T. Elsaesser, Localized multiphoton emission of femtosecond electron pulses from metal nanotips, Phys. Rev. Lett. **98**, 043907 (2007).
[22] J. W. Simonaitis, B. Slayton, Y. Yang-Keathley, P. D. Keathley, and K. K. Berggren, Precise, subnanosecond, and high-voltage switching enabled by gallium nitride electronics integrated into complex loads, Rev. Sci. Instrum. **92**, 074704 (2021).
[23] RoentDek Handels GmbH, WHAT RoentDek DETECTORS CAN (and cannot) DO, https://roentdek.com/products/guidelines/ (2023), online; accessed 5 December 2023.
[24] F. Read and N. Bowring, The CPO programs and the BEM for charged particle optics, Nucl. Instrum. Methods Phys. Res., Sect. A **645**, 273 (2011).
[25] H. Wollnik and M. Przewloka, Time-of-flight mass spectrometers with multiply reflected ion trajectories, Int. J. Mass Spectrom. Ion Process. **96**, 267 (1990).
[26] T. Y. Hirsh, N. Paul, M. Burkey, A. Aprahamian, F. Buchinger, S. Caldwell, J. A. Clark, A. F. Levand, L. L. Ying, S. T. Marley, G. E. Morgan, A. Nystrom, R. Orford, A. P. Galván, J. Rohrer, G. Savard, K. S. Sharma, and K. Siegl, First operation and mass separation with the CARIBU MR-TOF, Nucl. Instrum. Methods Phys. Res., Sect. B **376**, 229 (2016).
[27] D. Zajfman, O. Heber, L. Vejby-Christensen, I. Ben-Itzhak, M. Rappaport, R. Fishman, and M. Dahan, Electrostatic bottle for long-time storage of fast ion beams, Phys. Rev. A **55**, R1577 (1997).
[28] R. Shiloh, N. Schönenberger, Y. Adiv, R. Ruimy, A. Karnieli, T. Hughes, R. J. England, K. J. Leedle, D. S. Black, Z. Zhao, P. Musumeci, R. L. Byer, A. Arie, I. Kaminer, and P. Hommelhoff, Miniature light-driven nanophotonic electron acceleration and control, Adv. Opt. Photonics **14**, 862 (2022).
[29] R. Dahan, G. Baranes, A. Gorlach, R. Ruimy, N. Rivera, and I. Kaminer, Creation of optical cat and GKP states using shaped free electrons, Phys. Rev. X **13**, 031001 (2023).